Polish Society of Composite Materials
Polskie Towarzystwo Materiałów Kompozytowych

24: 3 (2024) 205-212

COMPOSITES THEORY AND PRACTICE

ISSN (online): 2299-128X

**Konstantin Nechval[1], Rafał Chatys[2], Igor Petukhov[1], Alexander Bain[1]**

[1] *Riga Aeronautical Institute, 9 Mežkalna, Riga LV-1058, Latvia*
[2] *Kielce University of Technology, Faculty of Mechatronics and Mechanical Engineering, al. 1000-lecia Państwa Polskiego 7, 25-314, Kielce, Poland*
**Corresponding author. E-mail:* chatys@tu.kielce.pl

*Received (Otrzymano) 10.05.2024*

# NEW APPROACH FOR AN INSPECTIONS PROGRAM AND USE OF C-FACTOR MODEL FOR STRESS ANALYSIS OF COMPOSITE COMPONENT STRUCTURE

https://doi.org/10.62753/ctp.2024.07.3.3

**A complete airplane structure is manufactured from many parts. These parts are made from sheets, extruded sections, forgings, castings, tubes, or machined shapes, which must be joined together to form subassemblies. The subassemblies must then be joined together to form larger assemblies and then finally assembled into a completed airplane. Many parts of the completed airplane must be arranged so that they can be disassembled for shipping, inspection, repair or replacement and are usually joined by bolts or rivets. In order to facilitate the assembly and disassembly of the airplane, it is desirable for such bolted or riveted connections to contain as few fasteners as possible (which is guaranteed by composite structures). Nevertheless, the impact of birds or elements during the take-off or landing (the operation) of an aircraft sometimes generates a critical dispersion of impact energy in the composite structure due to the high heterogeneity (of resin or microbubbles) of the structure. For example, a metal wing usually resists bending stresses in numerous stringers and sheet elements distributed around the periphery of the wing cross sections. The wing cannot be made as one continuous riveted assembly. The new approach to design an inspection scope and schedule based on maintenance checks brings elements of novelty. Although the maintenance schedule can be obtained through simulation, the simulation results might not be accurate enough. The obtained results provide usable analytical solutions. However, without an additional wide data-collection program, the results can serve only advisory purpose for practicians.**

**Keywords: aircraft riveted joints stress analysis, C-factor reliability**

## INTRODUCTION

An airplane construction is made of many complex structures. Each of them is manufactured from many single parts. These parts are made from sheets, extruded sections, forgings, and castings, which must be joined together solidly. The intermediate forms between the individual parts and the whole construction are the subassemblies, which must joined together to form larger assemblies and then finally assembled into a complete airplane. Many parts must be prepared to be disassembled for inspections, repairs or replacements. The parts are usually joined by bolts or rivets, which are problematic in the case of polymeric or composite structures. In order to facilitate the assembly and disassembly of the airplane, it is desirable that it contain as few fasteners as possible. Composite structures are usually deprived of joints. Nevertheless, the impact of birds or elements during the take-off or landing of an aircraft sometimes generates a critical dispersion of impact energy in the composite structure due to its high heterogeneity. In such case, often a whole part must be replaced, despite a the small damaged area. It is therefore advisable to use and assemble smaller parts in critical areas of the aircraft structure.

The main aim of the paper is to design an inspection scope and schedule of a construction or structure (e.g. a composite) to prevent catastrophic accidents. In many cases, during maintenance, some sections of the structure may have defects or pre-damage that need to be repaired with patches. For example, in the case of such patches, we can anticipate damage. However, we typically do not know in which places this structure will need to be fixed, but in some cases it could be defined by conditions due to loads acting on the structure. The performance of composite materials (structures) depends to a large extent on their strength, stiffness and integrity under specific operating conditions throughout their service life. Therefore, controlling the fracture process and predicting the durability of composite structures provides a reliable estimate of the quality of the produced components or products when exposed to different operating conditions.

## C-FACTOR MODEL FOR STRESS ANALYSIS

We consider the Tresca criterion [1, 2], one of two main failure criteria used today for ductile materials. The second important criterion is the von Mises criterion [3, 4].

The Trescae criterion specifies that a material would flow plastically according to this simple expression (1)

$$\sigma_{tresca} = \sigma_1 - \sigma_3 > \sigma_{\max} \tag{1}$$

The simplest comparison of the Tresca and von Mises criteria is shown in Figure 1 and later we can define a practical experiment with this concept.

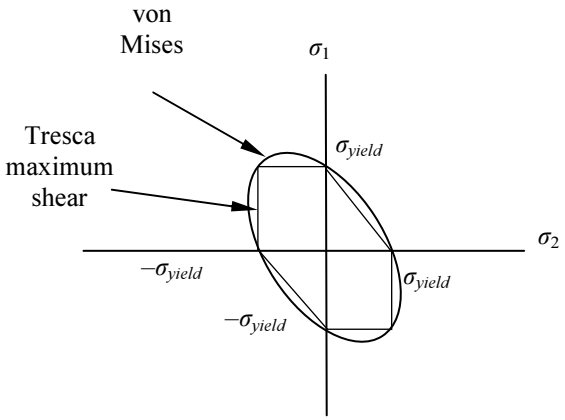


Fig. 1. Comparison of Tresca and von Mises criteria

When determining the strength of composite structures (especially in compression) using analytical methods, decreases in residual strength (as a result of exceeding the energy threshold) are observed as a consequence of an impact with various objects (e.g. birds) during aircraft take-off or landing, the extent of which depends on the inhomogeneity of the structure (resin or microbubbles) or the volume proportion of reinforcement in the composite [4]. Therefore, experimental methods have a special place in controlling and ensuring reliability in estimating the durability of manufactured composite products under different operating conditions of the fracture process in the composite structure.

The literature on the subject only discusses the quality of the description of the failure process and evaluates the probability of the extent of damage by analysing linear brittle failure mechanics criteria as equivalent Tresca and von Mises stresses (Fig. 2), or hydraulic pressure [4].

The next two questions concern the places where we can inspect this structure by the use of a probe and how we can do the check each time. In this method, we suppose that the range of frequencies will have an impact on the experimental results. The new approach in the paper is a C-factor model in which we can classify basic conditions for a special NDT method. We consider four main C-factor criteria:

C1 – the conditions of the fixed structure, and places for a probe.

C2 – the frequencies, tones and reference, levels of sound in dB.

C3 – the measurement system of Cartesian coordinates X, Y, Z and three angles α, β, γ. It helps to define the right axis of the ellipse and space orientation.

C4 – determination of structural changes or crack propagation.

Panels made from 2024 duralumin were used to form a frame of the structure. As can be seen in Figure 3, these panels consist of three ribs, one spar and a skin. In order to produce these parts fasteners, rivets and screws had to be used.

a)

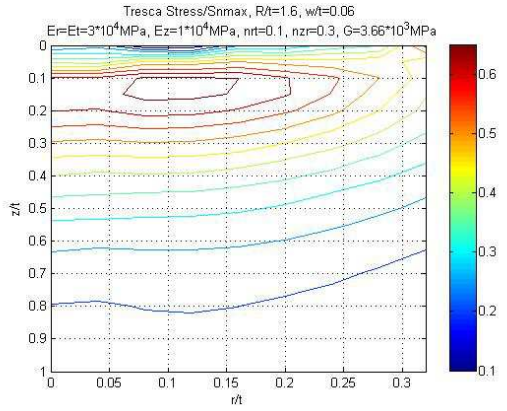


b)

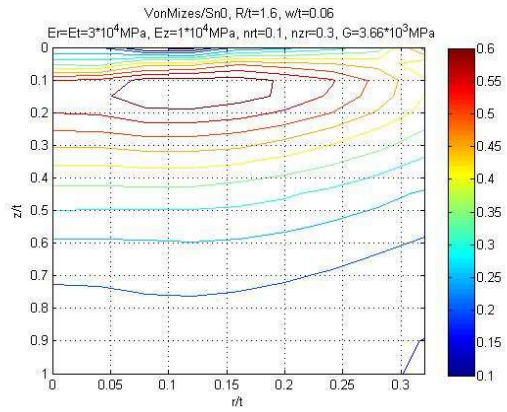


Fig. 2. Distribution of equivalent stresses in impact area as determined by Tresca (a) and von Mises (b) criteria: $R$, $t$ – width and thickness of composite; $w$ – depth of deformation after impact [4]

Fig. 3. Mounted joints, construction of ribs and rivets

 

First AutoCAD software was used to prepare a solid model of the assembled part. The generated model enables the C1 factor to be resolved. It needs to be noted that two panels can seem to be identical, but actually different shapes occur in the microscale and it is quite complicated to define small size deviations.

The appropriate software can detect the most significant points and later check the buckling of the part. For the basic conditions, we can choose the spar as the fixed support and other elements will be loaded with shear pressure. A number is assigned to each rivet as shown in Figure 4.

How can the most significant element in the structure be identified? The largest impact of the C1 factor occurs at locations of the connection between two probes. The modelling of the panels consists in defining points that have a high value of stress or could be at risk of significant loading. According to the model, we can assume that the highest danger points are situated on the right side of the rib (Fig. 4).

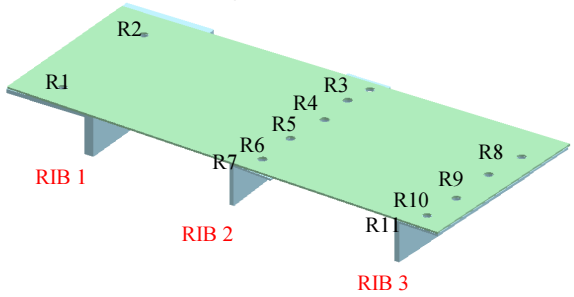


Fig. 4. Example of simple part and rivet (hole) numbers

An example analysis of the connection of the simple parts with neighbouring elements that have a minimum fatigue life margin is presented below. As can be seen in Figure 5, the connections associated with the minimum service life are located at rivets (R) numbered 3, 7, 8 and 11. Thus, an inspection is neccessary there.

In Figure 5 the point in red is the most appropriate location for the sensors and a probe.

The value of $\sigma R0$ for under loaded element connections made of Al-alloys (2024-T7451) for single-row fastening is 48.26 MPa, while the evaluated designed safe life of the element is 40 000 FH.

Now we consider a wave generator, which in our case is a source of dynamic input. Consequently, we move to the C2 criterion. In the areas of reliability and life testing, this problem translates to obtaining prediction intervals for life distributions such as the exponential and the Weibull distributions. For the Weibull case, several authors have addressed this issue as well as the more complicated problem of deriving prediction limits for order statistics from a future sample. These include Mann and Saunders [5].

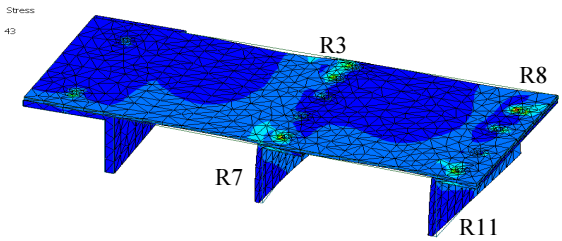


Fig. 5. Points of highest stress value

One of the earlier works on the prediction of the Weibull distribution is [5]. The authors considered prediction intervals for the smallest of a set of future observations, based on a small (consisting of two or three elements) preliminary sample of past observations. An expression for the warranty period (the time before the failure of the first ordered observation from a set of future observations) was derived as a function of the ordered past observations. Mann [5] extended the results for observation sizes $n$ = 10 (5) 25 and sample sizes $m$ = 2 (1) n-3 for a specified confidence level of 0.95. This method requires numerical integration. In addition, the commonly provided tables are limited to sample sizes of less than 25 and are given only for the confidence level of 0.95.

In the case of using composite structures, the bench (Fig. 6) must contain sensors with a built-in three-degree accelerometer, which is then connected via a controller to the lab view. The waves are generated by a special frequency generator with longitudinal and transverse waves, and the receiver registers an ellipse along three axes of the splash.

a)

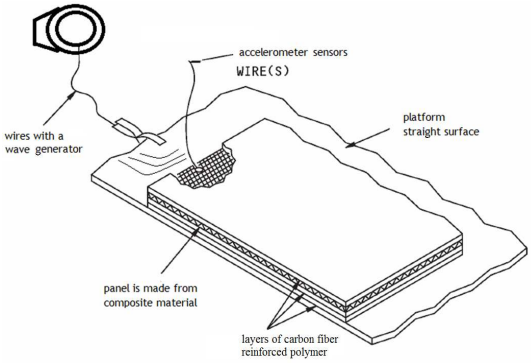


b)

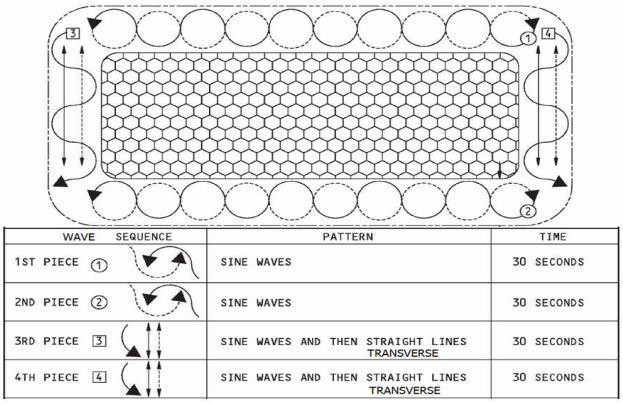


Fig. 6. Experimental setup constructed at Salford University: a) non-destructive testing of polymer-based component (composite structure); b) determination of wave type and frequency

Composites consist of a porous structure, usually a honeycomb structure. Such structures suppress wave energy very well, and therefore also provide sound and heat insulation. To bypass this counteraction effect, direct contact with the core of this structure is required and the waves must be of different types, as well as different frequencies. In the case of panels made from a composite structure consisting of three ribs, the frequency can be checked using acoustic emission methods [6, 7].

Investigations of specimens with a transverse arrangement of basic fibres (for the glass structure) in relation to tensile strength, Figure 7 illustates the two-stage nature of the deformation.

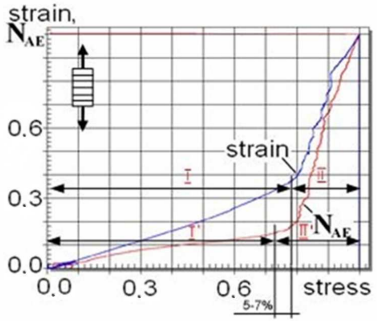


Fig. 7. Dependence of total acoustic emission and strain on stress of specimen with transverse fibre arrangement [8]

Both curves, related to the deformation and the acoustic emission parameter, are similar to the $\sigma$-$\varepsilon$ curve (Fig. 7), characterising the initial loading behaviour of the pure matrix (at $V_f = 0$, i.e. a matrix without the presence of reinforcement – fibres and weft fibres). In our case, the presence of the weft fibres, as the loading process takes place, leads to redistribution of the load, part of which is regrouped by the weft fibres and the warp, thus eliminating the initial stage. As can be seen in Figure 7, the process of irreversible deformation (the second stage of composite fracture) starts at about 0.8 of the breaking stress. Hence, in the first loading stage, the weft fibres are stretched, thus participating in the redistribution of the load to the matrix through elastic deformation. In the second stage, the limiting strength of the fibre or weft (as a group of so-called elementary fibre bundles) is reached. The intensity of the increase in total acoustic emission begins to rise. With further loading, the load is successively regrouped onto the remaining undamaged fibres or an elementary fibre bundle, leading to a further loss of strength of one or a number of wefts.

The increase in the intensity of the total acoustic emission continues to grow. The further increase in strain is apparently due to the self-destruction process. From this point onwards, the strain parameter, as can be seen in Figure 7, starts to grow more intensively than the stress. The rapid rise in both parameters results in complete destruction of the specimen cross-section. Therefore, the process of the initiation of composite destruction under this type of loading is detected from the acoustic emission data 5 % - 6 % earlier than indicated by the strain parameter, as confirmed in [7, 8].

## DATA AND METHODS

Antle and Rademaker [9] provided a method of obtaining a prediction for the largest number of observations from a future sample of a Type I extreme value distribution, based on the maximum likelihood estimates of the parameters. They used Monte Carlo simulations to obtain the prediction intervals. Using the well-known relationship between the Weibull distribution and the Type I extreme value distribution, one can use their method to construct an upper prediction limit for the largest one among a set of future Weibull observations. However, this method is valid only for complete samples and limited to constructing an upper prediction limit for the largest one among a set of future observations.

The distribution theory for the estimators of unknown parameters in Weibull models is complicated and cannot be described in explicit forms. Nevertheless, by using a conditional method, many problems become analytically manageable. The conditional method used in this paper is one conditioned by ancillary statistics, which was first suggested by Fisher [10] and promoted further by a number of other authors (Cox [11], Buehler [12]). Lawless [13] applied this conditional method to different problems relating to the Weibull and extreme value distributions.

In the conditional method, the quantiles for the construction of prediction intervals depend on ancillary statistics of observed data. This procedure, in which the results are based on the conditional distribution of the maximum likelihood estimates given as a set of ancillary statistics is exact, but it requires numerical integration for each new obtained sample in order to determine the prediction limits.

## EQUATION FOR CONSTRUCTING SIMULTANEOUS PREDICTION LIMIT

The method of constructing prediction limits for future samples from a Weibull distribution (2) introduced in this paper utilizes all the information about a sample, but since it involves the use of numerical integration, many may prefer to use this technique only in situations not readily handled by other methods described earlier.

$$\Pr\{Y_1 > \tau_j;\mathbf{z}\} = \Pr\left\{\hat{\delta}\ln\left(\frac{Y_1}{\hat{\beta}}\right) > \hat{\delta}\ln\left(\frac{\tau_j}{\hat{\beta}}\right);\mathbf{z}\right\} = \Pr\{W_1 > w_{j,(1-\alpha)};\mathbf{z}\}$$
$$= \frac{\int_0^\infty v^{r-2} e^{v\hat{\delta}\sum_{i=1}^{r}\ln(x_i/\hat{\beta})}\left(me^{vw_{j,(1-\alpha)}} + \sum_{i=1}^{r} e^{v\hat{\delta}\ln(x_i/\hat{\beta})} + (n-r)e^{v\hat{\delta}\ln(x_r/\hat{\beta})}\right)^{-r} dv}{\int_0^\infty v^{r-2} e^{v\hat{\delta}\sum_{i=1}^{r}\ln(x_i/\hat{\beta})}\left(\sum_{i=1}^{r} e^{v\hat{\delta}\ln(x_i/\hat{\beta})} + (n-r)e^{v\hat{\delta}\ln(x_r/\hat{\beta})}\right)^{-r} dv}$$
$$= (1-\alpha)^j, \quad j \geq 1 \qquad (2)$$

 

With modern computing, however, the conditional prediction limits are not difficult to calculate and should be recommended when the ability to do computations is available [13, 14].

The proposed technique may be useful when we consider, for example, the reliability problem associated with fatigue damage that arises from the initiation of fatigue cracks originating from rivet holes along the top longitudinal row of the outer skin of the panel [13].

## PRACTICE AND EXPERIMENT

An experiment was set up with an instrument system and special software as a part of new NDT method development, and no further confidential information could be given to conform to "know how".

During calibration, we chose the most effective frequency – 258 Hz (Fig. 8), but in other experiments it could be possible to use other frequencies. It was determined based on the application points as shown in Figure 5. Nonetheless, the method of choosing such a value of frequency and other parameters is defined as top secret.

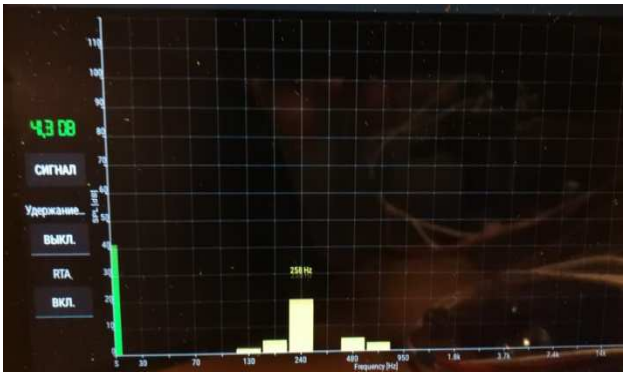


Fig. 8. Resolved frequencies of about 258 Hz

If the frequency is generated by two or more sources, an ellipse axis as a dependence of the wave longitude will be observed. It should be noted that this “ellipse dancing” can explain the impact of interference and, as a result, could possibly identify an initial microfracture. Further experiments must be conducted to investigate this effect (Fig. 8). In this experiment some special equipment is used.

In order to interpret the results, we must have default values of the initial settings for the calibration instruments that can help identify fracture effect overlapping with shape and reliable comparison. The next figure (Fig. 9) shows some small deflection due to non-destructive testing. In the subsequent step a decision needs to be made to prevent some maintenance or resolve small defects. The sensors of the accelerometers provide information seen on the laptop screen.

This non-destructive testing method is relatively new and good results can be obtained by combining it with the resource test assignment method.

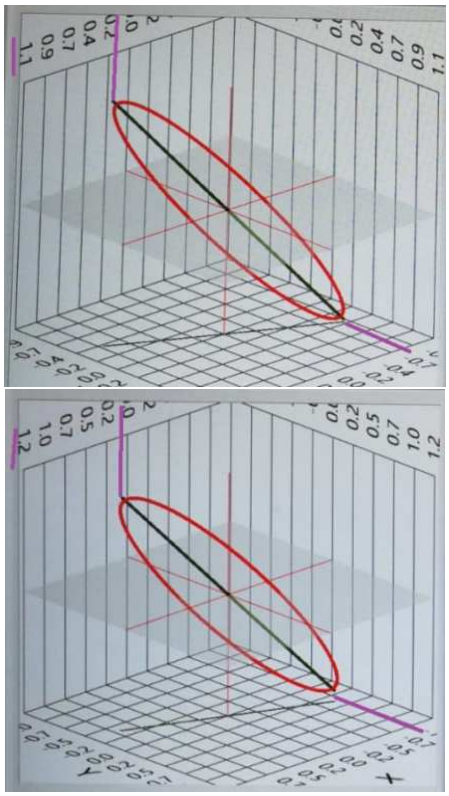

Fig. 9. Results of experiment at frequency of 258 Hz and free of payment loads

## MAINTENANCE AND RELIABILITY

In many cases, during maintenance some sections could have fails or pre-fails that must be repaired with patches. Table 1 shows several time intervals regarding such patches, which we can predict in this experiment.

TABLE 1. **Crack initiation in calculated time intervals [15]**

| $w_j$ | **Inspection time $\tau_j$ ($\times 10^4$ flight hours)** | **Interval $\tau_{j+1} - \tau_j$ (flight hours)** |
|---|---|---|
| – | $\tau_0 = 0$ | – |
| $w_1 = -8.4378$ | $\tau_1 = 2.5549$ | 25549 |
| $w_2 = -6.5181$ | $\tau_2 = 3.2569$ | 7020 |
| $w_3 = -5.5145$ | $\tau_3 = 3.6975$ | 4406 |
| $w_4 = -4.8509$ | $\tau_4 = 4.0212$ | 3237 |
| $w_5 = -4.3623$ | $\tau_5 = 4.2775$ | 2563 |
| $w_6 = -3.9793$ | $\tau_6 = 4.4898$ | 2123 |
| $w_7 = -3.6666$ | $\tau_7 = 4.6708$ | 1810 |
| $w_8 = -3.4038$ | $\tau_8 = 4.8287$ | 1579 |
| $w_9 = -3.1780$ | $\tau_9 = 4.9685$ | 1398 |
| ⋮ | ⋮ | ⋮ |

Aircraft maintenance checks are periodic inspections that have to be done on all commercial/civil aircraft after a certain amount of time or usage. Airlines and other commercial operators of large or turbine-powered

 

aircraft follow a continuous inspection program approved by the Federal Aviation Administration (FAA) in the United States or by other airworthiness authorities such as Transport Canada or the European Aviation Safety Agency (EASA). Under FAA oversight, each operator prepares a Continuous Airworthiness Maintenance Program (CAMP) under its Operations Specifications or "OpSpecs". CAMP includes both routine and detailed inspections. Airlines and airworthiness authorities casually refer to the detailed inspections as "checks", commonly one of the following: A check, B check, C check, or D check. A and B checks are less intensive checks, while C and D are considered more intensive checks.

It needs to be noted that the following example of using the latest inspection scope and schedule is a new method which incorporates a great deal of research, hence without the previous articles of the authors, it will be difficult for a beginner to understand. Once again, it has to be remembered that this is just an example of research and does not have to be the reality of numbers and data − everything is obtained as a result of calculations. One does not need to refer to a specific aircraft type, but to a generalized criterion. All the calculated intervals that will be summarized in the maintenance check form are given in Figure 9. Below we have chosen these forms only to illustrate this graph; how it could look in reality depends on the maintenance planning engineer, as shown in Figure 10.

*Weekly check* – Some of the scheduled or routine maintenance tasks stated in the maintenance schedule could be listed together in a consolidated check sheet, which are called up in a transit check with a longer ground time. The complete package is sometimes referred to as a complete overhaul cycle. The concept is called block maintenance or sometimes progressive maintenance. A weekly check is required about every 36 flight hours, depending on the aircraft.

*A check* – Consists of a visual examination of the airframe, engines, avionics, and accessories to ascertain the general condition of the aircraft, for about (8) eight hours on the ground. The A check is performed approximately every month (500 flight hours), or every 200-300 flights (cycles), depending on the aircraft type. This check takes about 50-70 man-hours, and is usually performed in an airport hangar.

*B check* – A similar schedule applies to the B check as to the A check. However, B checks may also be incorporated into successive A checks, i.e. checks A-1 through A-2 complete all the B check items. It includes the A check plus selected operational checks, fluid servicing and lubrication as well as an open inspection of the panels and cowlings. It is about 24 hours of ground time. The B check is performed approximately every 6 months or every 1000 flight hours, depending on the aircraft. This check takes about 160-180 man-hours, depending on the aircraft, and is usually completed within 1-3 days at an airport hangar.

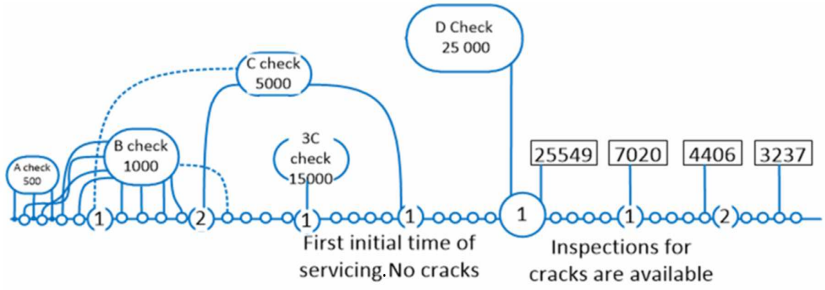


Fig. 9. Example of inspection schedule

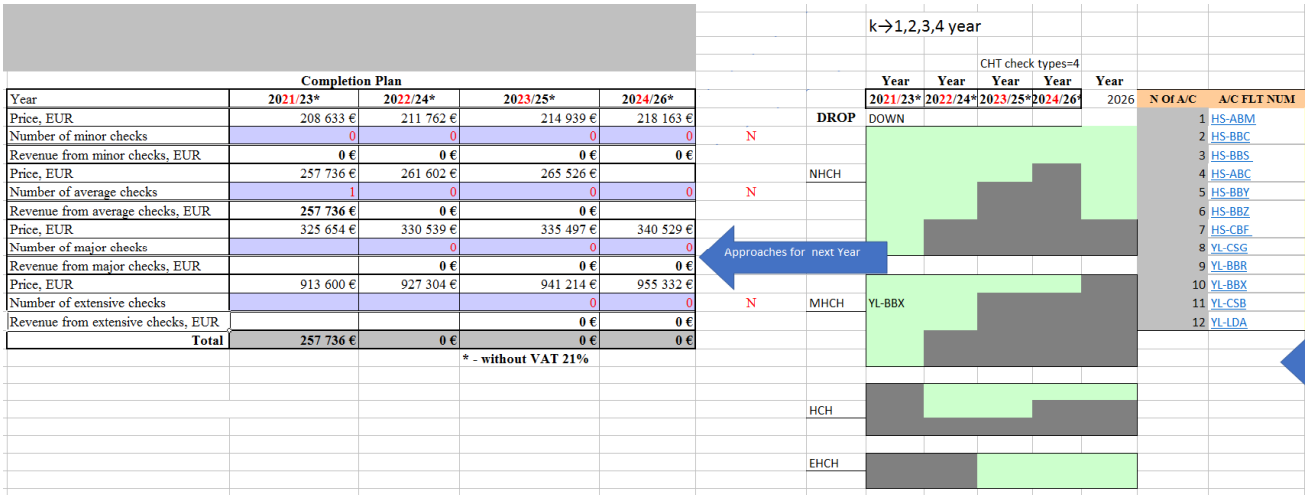

| Completion Plan | | | | |
|---|---|---|---|---|
| Year | 2021/23* | 2022/24* | 2023/25* | 2024/26* |
| Price, EUR | 208 633 € | 211 762 € | 214 939 € | 218 163 € |
| Number of minor checks | 0 | 0 | 0 | 0 |
| Revenue from minor checks, EUR | 0 € | 0 € | 0 € | 0 € |
| Price, EUR | 257 736 € | 261 602 € | 265 526 € | |
| Number of average checks | 1 | 0 | 0 | 0 |
| Revenue from average checks, EUR | 257 736 € | 0 € | 0 € | |
| Price, EUR | 325 654 € | 330 539 € | 335 497 € | 340 529 € |
| Number of major checks | | 0 | 0 | 0 |
| Revenue from major checks, EUR | | 0 € | 0 € | 0 € |
| Price, EUR | 913 600 € | 927 304 € | 941 214 € | 955 332 € |
| Number of extensive checks | | | 0 | 0 |
| Revenue from extensive checks, EUR | | | 0 € | 0 € |
| Total | 257 736 € | 0 € | 0 € | 0 € |

* - without VAT 21%



Fig. 10. New approach to assign maintenance schedule for inspections of base maintenance checks

 

*C check* – This maintenance check is much more extensive than a B check, requiring a majority of the aircraft's components to be inspected. This check puts the aircraft out of service and until it is completed; the aircraft must not leave the maintenance site. It also requires more space than A and B checks. It is therefore usually carried out in a hangar at a maintenance base. It includes the A and B checks plus detailed inspection of the airframe, engines and accessories, thorough lubrication, and a portion of the corrosion prevention program. The flight controls are calibrated, major internal mechanisms are tested and the Service Bulletin requirements are fulfilled. It is about 72 hours of ground time. The C check is performed approximately every 24 months or every 5000 flight hours, depending on the aircraft. The time needed to complete such a check is generally 1-2 weeks and the effort involved can require up to 3000 man-hours.

*3C check*, or Intermediate Layover (IL) – Some authorities use this type of check, which typically includes light structural maintenance, and checks for corrosion on specific high-load parts of the airframe. The 3C check may also be used as the opportunity for cabin upgrades, e.g. new seats, entertainment systems or carpeting. This shortens the time the aircraft is out of service by performing two distinct tasks simultaneously. As component reliability has improved, some maintenance repair organizations (MROs) now spread the workload across several C checks, or incorporate this 3C check into D checks instead. The 3C check is performed approximately every 6 years or every 15000 flight hours, depending on the aircraft.

*D check* – It is a check that more or less takes the entire airplane apart for inspection and overhaul. Even the paint may need to be completely removed for further inspection of the fuselage metal skin. It also requires the most space of all maintenance checks, and as such must be performed at a suitable maintenance base. The requirements and the tremendous effort involved in this maintenance check make it by far the most expensive, with total costs for a single visit ending up well within the million-dollar range. This check occurs approximately every 10 years or every 25 000 flight hours. Such a check can generally take up to 10 000 man-hours and 2 months to complete, depending on the aircraft and the number of technicians involved and about 21 days of ground time.

If the flows of probable failures of certain structural units are well known, together with combining and adding different inspection periods into a common form of maintenance, we can use the program to assign forms for various types of aircraft (as shown in Fig. 10). The inspection plans for the specific hot spots (riveted holes) are determined from the generic inspection plans by the methods mentioned before. This requires a user-interface where the generic parameters of the specific values according to Weibull distribution can be entered and stored, and where the resulting inspection plans together with their expected costs are provided in a suitable format. A standard spreadsheet format is used to plan these tasks because of its flexibility and because it allows one to make the calculation procedures transparent. In addition, most engineers are familiar with these formats. Because computational performance is not crucial here, all the functions are computed in Excel. The figure below provides an overview of the developed tool (iTables.xls).

At the same time, there is no need for a reliable history of events; we can model the service flows of various aircraft, knowing only the year they were put into operation.

The example demonstrates the use of Poisson's law to assign event flows to maintenance forms. How the presented schedule is used and what a maintenance program might look like will be the subject of a subsequent paper, together with some new information on this subject.

## CONCLUSIONS

In the current age of technology it is very difficult to find something new, but this attempt brings elements of novelty. Although the results of this paper can be obtained through simulation, the simulation may not be accurate enough. From the theoretical as well as practical points of view, analytical solutions should be used if they are available. The results of this paper provide such analytical solutions.

In addition, the methods employed in this article can be applied to obtain practical data, but this already requires extensive interaction with engineers. The concept of free research and obtaining analytical data serve only an advisory purpose for engineers.

## REFERENCES

[1] Christensen R.M., The failure theory for isotropic materials: Proof and completion, Journal of Applied Mechanics 2020, 87(5), 051001.

[2] Cunha A. Jr, Yanik Y., Olivieri C., da Silva S., Tresca vs. von Mises: Which failure criterion is more conservative in a probabilistic context? Journal of Applied Mechanics 2023, in press. hal-04245274 (https://hal.science/hal-04245274).

[3] Ding B., Li X., An eccentric ellipse failure criterion for amorphous materials, Journal of Applied Mechanics 2017, 84(8), 081005.

[4] Pavelko V.P., Pavelko I.W., Chatys R., Strength of fibrous composites with impact damage, VI Conf. Polymer Composites, 24-26.11.2007, Wisła (Poland), Prace Naukowe Politechniki Warszawskiej, Mechanika 2007, 219, 187-198.

[5] Man N.R., Saunders S.C., On evaluation of warranty assurance when life has a Weibull distribution, Biometrika 1969, 56, 615-625.

[6] Urbahs A., Banovs M., Turko V., Feshchuk Y., New approach to use the acoustic emission monitoring for the defects detection of composit-material's design elements, Water Transport and Infrastructur: 14. Inter. Konference, Latvia, Riga 2012, April, 26-27, 45-50.

[7] Banov M.D., Pogorodny P.G., Shestakov V., Chatys R., Quantum approach in the measurement and analysis of

acoustic emission signals, AIP Conference Proceedings, Scientific Session on Applied Mechanics X, Bydgoszcz 2019, 22-30, DOI: 10.1063/1.5091867.

[8] Mann N.R., Warranty periods based on three ordered sample observations from a Weibull population, IEEE Transactions on Reliability 1970, R-19, 167-171.

[9] Antle C.E., Rademaker F., An upper confidence limit on the maximum of m future observations from a Type 1 extreme-value distribution, Biometrika 1972, 59, 475-477.

[10] Fisher R.A., Two new properties of mathematical likelihood, Proceedings of the Royal Society A 1934, 144, 285--307.

[11] Cox D.R., Some problems connected with statistical inference, The Annals of Mathematical Statistics 1958, 29, 357-372.

[12] Buehler R.J., Some validity criteria for statistical inferences, The Annals of Mathematical Statistics 1959, 30, 845-863.

[13] Lawless J.F., Statistical Models and Methods for Lifetime Data, John Wiley, New York 1982.

[14] Dąbek L., Kapjor A., Orman Ł.J., Ethyl alcohol boiling heat transfer on multilayer meshed surfaces, Proc. 20th Int. Scientific Conference on The Application of Experimental and Numerical Methods in Fluid Mechanics and Energy 2016, AIP Conference Proceedings 2016, 1745, 020005, DOI: 10.1063/1.4953699.

[15] Nečvals K., Petuhovs I., Assigning warranty periods for fatigue sensitive components of aircraft structure, Proceedings of the 6th International Scientific and Practical Conference Transport, Education, Logistics and Engineering – 2021, 13-27.